Personalized Rescheduling of Adaptive Organ-at-Risk-Sparing Radiation Therapy for Head and Neck Cancer under Re-planning Resource Constraints: A Novel Application of Markov Decision Processes

Fatemeh Nosrat[1,†], Cem Dede[2,‡], Lucas B. McCullum[2,3,‡], Raul Garcia[1,†], Abdallah S. R. Mohamed[2,4,‡], Jacob G. Scott[5], James E. Bates[6], Brigid A. McDonald[2,‡], Kareem A. Wahid[2,‡], Mohamed A. Naser[2,‡], Renjie He[2,‡], Amy C. Moreno[2,‡], Lisanne V. van Dijk[2,7], Kristy K. Brock[8], Jolien Heukelom[9], Seyedmohammadhossein Hosseinian[10,†], Mehdi Hemmati[11,†], Andrew J. Schaefer[1,†], Clifton D. Fuller[1,2,†,‡], on behalf of the Rice/MD Anderson Center for Operations Research in Cancer (CORC)[†] and the MD Anderson Head and Neck Cancer Symptom Working Group[‡]

[1]Department of Computational Applied Mathematics and Operations Research, Rice University, Houston, TX, USA
[2]Department of Radiation Oncology, The University of Texas MD Anderson Cancer Center, Houston, TX, USA
[3]The University of Texas MD Anderson Cancer Center UTHealth Houston Graduate School of Biomedical Sciences, Houston, TX, USA
[4]Department of Radiation Oncology, Baylor College of Medicine, Houston, TX, USA
[5]Department of Translational Hematology and Oncology Research, Lerner Research Institute, Cleveland, OH, USA
[6]Department of Radiation Oncology, Emory University, Atlanta, GA, USA
[7]Department of Radiation Oncology, University of Groningen, University Medical Center Groningen, Groningen, Netherlands
[8]Department of Imaging Physics, The University of Texas MD Anderson Cancer Center, Houston, TX, USA
[9]Department of Radiation Oncology (Maastro), GROW School for Oncology and Reproduction, Maastricht University Medical Centre+, Maastricht, Netherlands
[10]Department of Mechanical and Materials Engineering, University of Cincinnati, Cincinnati, OH, USA
[11]School of Industrial and Systems Engineering, University of Oklahoma, Norman, OK, USA
Corresponding Author: Fatemeh Nosrat (`fatemeh.nosrat@rice.edu`)
Co-Corresponding Authors: Andrew J. Schaefer, Clifton D. Fuller

1 April 2024

Data availability statement: The anonymized data from the enclosed manuscript

has been deposited at DOI:10.6084/m9.figshare.25517338.

Funding statement: This work was supported by the National Institutes of Health (NIH) National Cancer Institute (NCI) Research Grant (R01CA257814), the NCI Cancer Center Support Grant Program in Image-Driven Biologically-informed Therapy (IDBT) Program (P30CA016672), and the Image Guided Cancer Therapy Research Program at The University of Texas MD Anderson Cancer Center, and the MD Anderson Charles and Daneen Stiefel Center for Head and Neck Cancer Oropharyngeal Cancer Research Program. Lucas B. McCullum and Raul Garcia were supported by the NCI Supplement program under R01CA257814-02S2, and R01CA257814-03S2, respectively. Drs. McDonald and Wahid are both supported by the Image-guided Cancer Therapy T32 Fellowship (T32CA261856). Dr. Heukelom received related support from the Netherlands Rene Vogels Fond Fellowship. Drs. Heukelom and van Dijk received relevant support from the Dutch Cancer Society/KWF Kankerbestrijding. Dr. Fuller received related support from the National Institute of Dental and Craniofacial Research (NIDCR) (R01DE028290). Dr. Fuller has received related direct industry grant/in-kind support, honoraria, and travel funding from Elekta AB. Dr. Fuller has served in an unrelated consulting capacity for Varian/Siemens Healthineers. Philips Medical Systems, and Oncospace, Inc. Dr. Brock received unrelated support from the Helen Black Image Guided Fund, RaySearch Laboratories AB, the Apache Corporation,and the Tumor Measurement Initiative through the MD Anderson Strategic Initiative Development Program (STRIDE) and various NIH mechanisms. Dr. Scott received relevant support under the NCI Case Comprehensive Cancer Center Support Grant (P30CA043703), with additional unrelated NIH support. Dr. Moreno received related support from NIDCR (K01DE030524) and NCI (K12CA088084) during the project period, with additional unrelated NIH support.

Abstract.

Objective. The objective of this study was to determine personalized optimal timing for re-planning in adaptive organ-at-risk-sparing radiation therapy under limited re-planning resources in patients with head and neck cancer (HNC).

Approach. A novel Markov decision process (MDP) model was developed to determine optimal timing of re-plannings based on the patient's expected toxicity, characterized by normal tissue complication probability (NTCP), for four toxicities: xerostomia, dysphagia, parotid gland dysfunction, and feeding tube dependency at 6 months post-treatment. The MDP parameters were derived from a dataset comprising 52 HNC patients treated at the University of Texas MD Anderson Cancer Center between 2007 and 2013. Optimal re-planning strategies were obtained when the permissible number of re-plannings throughout the treatment was limited to 1, 2, and 3.

Main results. The MDP (optimal) solution recommended re-planning when the difference between planned and actual NTCPs (ΔNTCP) was greater than or equal to 1%, 2%, 2%, and 4% at treatment fractions 10, 15, 20, and 25, respectively, exhibiting a temporally increasing pattern. The ΔNTCP thresholds remained constant across the number of re-planning allowances (1, 2, and 3). This result underscores the importance of re-planning for patients experiencing the slightest change in ΔNTCP at fraction 10.

Significance. In contrast to prior work that relies on a single re-planning allowance

or predetermined time intervals using a one-size-fits-all approach, the MDP model proposed in this paper offers a personalized, resource-aware, and scalable decision-making tool; it identifies optimal dynamic re-planning schedules tailored to individual needs, guided by changes in NTCP.

Keywords: Personalized adaptive radiation therapy, organs-at-risk, normal tissue complication probability, Markov decision process, optimal strategy

1. Introduction

Advancements in radiation delivery techniques, such as intensity-modulated radiation therapy (IMRT) and volumetric-modulated arc therapy, enable accurate dose delivery to tumor targets while minimizing radiation exposure of the surrounding organs-at-risk (OARs) [1]. However, anatomical changes during the treatment, such as weight loss or tumor shrinkage, may cause the actual delivered dose to OARs to deviate from the planned dose. This can increase the risk of treatment-induced toxicities, particularly in cases where multiple OARs are in close proximity to the target, as in head and neck cancer (HNC) [2, 3, 4]. To address this, adaptive radiation therapy (ART) is clinically introduced, proposing on-therapy re-planning in response to anatomical changes in the target and OARs [5, 6, 7, 8, 9, 10].

The unmet need in ART revolves around the finite availability of crucial resources to perform key tasks such as segmentation and quality assurance that, together with limited device time, results in the impracticality of daily re-plannings with current technologies [11, 12]. Recent advancements in artificial intelligence-based algorithms promise streamlining certain tasks (e.g., auto-segmentation); however, their integration into current ART workflow is still evolving and requires further refinement for widespread clinical application [13]. Thus, determining the optimal timing of re-plannings under limited resources remains a challenge [14, 15]. This challenge extends to the uncertainty regarding the optimal frequency of re-plannings, with historical work often relying on a fixed number of re-plannings and/or fixed-interval re-plannings [14, 15]. Moreover, the literature presents conflicting evidence on the value of single or multiple re-plannings, as exemplified by studies like Abou-Alfa et al. [16] and Castelli et al. [17]; while Castelli et al. [17] found no improvement with a single re-planning, Abou-Alfa et al. [16] showed enhancement with a single re-planning, emphasizing the need for further research.

In the context of hybrid MR-linac (MRL) as a compelling use case in radiation therapy, ART becomes a critical aspect, especially considering that MR-linacs enable on-line ART, allowing for real-time adjustments to treatment plans based on patient anatomy or tumor response. On-line ART can also be enabled with the availability of high-frequency, high-quality cone-beam CT, e.g., through the recently introduced Varian Ethos system [18, 19]. Additionally, CT-on-Rails, with the ability to offer precise imaging with less logistical constraints, presents an alternative option to implement

ART, particularly for centers with access to CT-based data for treatment re-planning. Cancer centers in the US, guided by institutional protocols, typically advocate for ART at fixed-interval times, notably once mid-therapy [20]. However, such guidelines implement a one-size-fits-all approach and do not account for uncertain trajectory of the toxicities that an individual may experience [21]. Whether in the MRL context, especially when not adapting the gross tumor volume (GTV) as explored in the MR-ADAPTOR trial [22], or in CT-based non-GTV-adaptive approaches [16, 17], the practical consideration of 're-planning allowance' becomes paramount in optimal decision making. The main challenge in finding the optimal timing of re-plannings at the individual level lies in the uncertainty of anatomical changes during the treatment.

Heukelom et al. [21] investigated the optimal implementation of ART with a single re-planning allowance (in OAR-sparing radiation therapy) using daily on-treatment CT imaging with a CT-on-rails device. Leveraging the same dataset, this paper presents a new analytical approach for optimal re-planning strategies, based on Markov decision process (MDP) models, to identify the optimal timing for re-planning under different allowances in HNC. MDPs constitute a class of mathematical optimization models that aim to determine optimal decisions/actions in stochastic dynamic systems [23, 24]. MDPs are extensions of Markov models, which capture the natural evolution of a stochastic process (e.g., cancer progression) and are more commonly used in cancer research [25, 26, 27]. MDPs incorporate possible interventions (actions) into the stochastic process with the aim of obtaining desired outcomes at the end of a time horizon, by identifying an optimal course of actions. MDPs have been successfully employed to find the optimal timing for various medical interventions [27, 28, 29, 30, 31]; however, to our knowledge, MDPs have not been applied for triggering adaptive re-planning. By leveraging a mathematically optimal and rigorous decision process, we propose a method for evidence-based individualized radiation treatment re-planning, scalable across resource-rich and resource-limited facilities, and applicable to both CT- and MR-based platforms. Thus, rather than a class solution based on population estimates of toxicity reduction potential, we enable personalized adaptive therapy with awareness of a budget.

This study undertakes three specific aims: 1) Develop a generalized framework for the utilization of MDPs in budgeted re-planning decisions for efficient resource allocation in clinical settings, 2) identify the optimal timing of re-plannings based on changes in normal tissue complication probabilities (NTCP) of four toxicities: xerostomia, dysphagia, parotid gland dysfunction, and feeding tube dependency at 6 months post-treatment to enhance personalized treatment and efficacy, and 3) provide a foundation for future research efforts, which could extend the application of these methodologies to more dynamic treatment scenarios, such as GTV adaptive and/or online adaptive workflows, with the goal of achieving sufficient speed and flexibility for real-time clinical decision making. Through these aims, we seek to not only refine the strategic application of ART but also to contribute to the broader discourse on improving cancer treatment outcomes through mathematical modeling and optimization.

2. Materials and Methods

2.1. Data

This study uses a prior dataset of CT-on-Rails image-guided radiation therapy (IGRT), detailed by Heukelom et al. [21], which comprises information from patients treated for HNC at the University of Texas MD Anderson Cancer Center between 2007 and 2013; this retrospective secondary analysis was performed under MD Anderson Cancer Center Institutional Review Board approval (MDA RCR03-0800). The treatments involved (chemo-) radiotherapy with daily CT-on-Rails IGRT. Of the 52 patients, 36 were male and 16 were female. Among them, 46 patients were aged 18-65, while the remaining 6 were older than 65. The primary cancer sites were as follows: Larynx (1 patient), Oropharynx (13), Oral cavity (4), Hypopharynx (0), Nasopharynx (15), and Sinonasal (12). Treatment modalities included radiotherapy alone (16 patients), induction chemotherapy followed by radiotherapy (2), induction chemotherapy followed by concurrent chemoradiation (16), concurrent chemoradiation (14), and radiation plus Cetuximab (4). The patients' characteristics are summarized in table 1.

For these 52 HNC patients, Heukelom et al. [21] calculated deviation of the actual dose from the planned dose for nine OARs at fractions 10 and 15 of the treatment. At each fraction, they estimated NTCP for the toxicities related to the OARs (xerostomia, dysphagia, parotid gland dysfunction, and tube feeding dependency at 6 months post-treatment) by projecting the actual dose through the remainder of the treatment period. Subsequently, they compared these findings with the planned NTCPs and determined the difference, i.e., ΔNTCP, for each toxicity. The NTCP models are presented in Appendix A. For each observed ΔNTCP value, they reported the number of patients exhibiting that ΔNTCP or higher in any of the four NTCP models. The MDP model presented in this paper uses the ΔNTCP from this dataset [21], which are summarized in table 2.

2.2. Decision Model

In the MDP model, estimates of an individual patient's toxicity outcome, as a function of the delivered radiation dose to OARs, determine the state of the system at each decision epoch during the treatment (e.g., day). Depending on the observed state, the clinician may decide between two possible actions: (1) Re-plan or (2) continue with the current plan. When the action is to continue with the current plan, the system may transition from one toxicity state to another stochastically, governed by transition probabilities. Re-planning changes the probabilistic transition towards more favorable outcomes/states. Given that a limited number of 're-planning' actions may be taken throughout the treatment, an optimal solution to the MDP identifies the optimal timing for taking such actions, as a function of the toxicity states. Figure 1 illustrates an overview of the analysis method.

The MDP model captures the stochastic evolution of post-treatment toxicity risk

Table 1: Patient characteristics. Abbreviations: cCRT = concurrent chemoradiation. RT = radiotherapy. TNM classification according to version 3. Accelerated RT: 2 Gy per fraction, 6 times per week.

Variable	Number of Patients = 52	
Sex	Male	69%
	Female	31%
Age	18-65 years	88%
	$\geq$ 65 years	12%
T-classification	Tis-T1	8%
	T2	15%
	T3	13%
	T4	54%
	Recurrence	8%
	Unknown	2%
	Post-surgery	23%
N-classification	N0	27%
	N1	19%
	N2	38%
	N3	2%
Primary site	Larynx	2%
	Oropharynx	25%
	Oral cavity	8%
	Hypopharynx	0%
	Nasopharynx	29%
	Sinonasal	23%
Pathology	Adenocarcinoma	2%
	Neuroblastoma	6%
	Neuroendocrine	8%
	Squamous cell carcinoma	50%
	Undifferentiated carcinoma	17%
	Other	17%
Treatment modality	Radiotherapy alone	31%
	Induction chemotherapy followed by RT	4%
	Induction chemotherapy followed by cCRT	31%
	Concurrent chemoradiation	27%
	Radiation + Cetuximab	8%
Baseline weight loss	No weight loss	38%
	Moderate weight loss (1 – 10%)	33%
	Severe weight loss (>10%)	6%
	Unknown	23%
Baseline xerostomia	No xerostomia	4%
	Some xerostomia	8%
	Unknown	88%
Accelerated RT	Yes	6%

Table 2: Observed ΔNTCP values based on the difference between planned dose and actual dose, along with the number of patients associated with each ΔNTCP value. Adapted from [21] with permission.

(a) Fraction 10

ΔNTCP	0%	1%	2%	3%	4%	5%	6%	7%	8%	9%	10%	11%	12%
Number of Patients	26	7	4	6	2	2	0	1	0	0	1	1	2

(b) Fraction 15

ΔNTCP	0%	1%	2%	3%	4%	5%	6%	7%	8%	9%	10%	11%	12%
Number of Patients	23	8	9	2	2	1	1	2	0	0	2	1	1

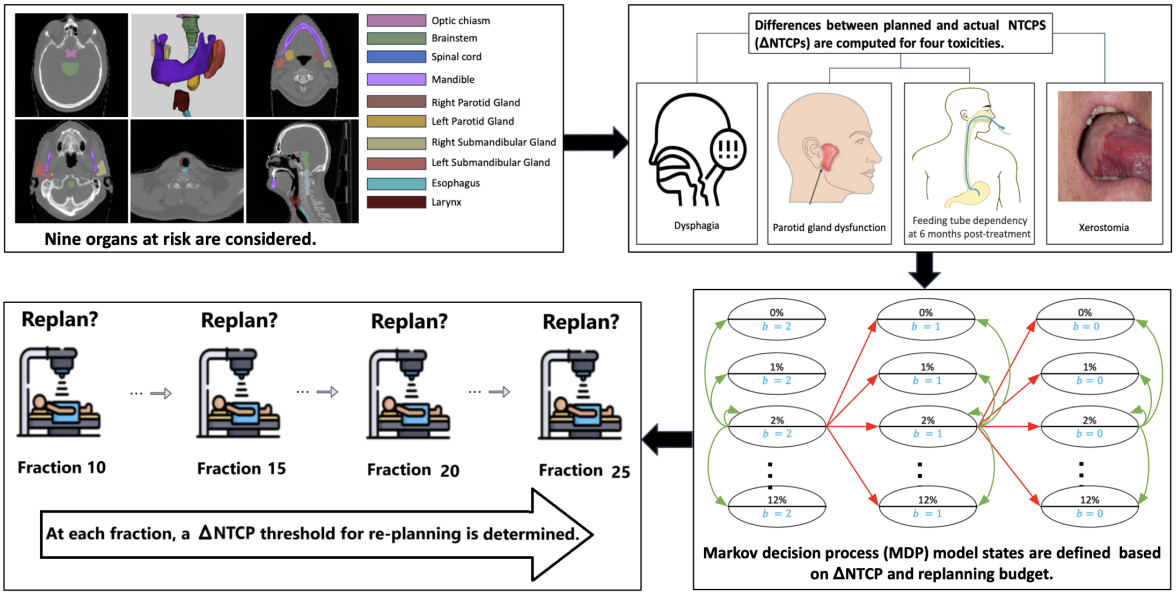

Figure 1: Overview of the analysis method. The sub-figures displaying OARs and toxicities are adapted from [32] with permission.

and identifies optimal re-planning times to mitigate the toxicities (if necessary). The model components are as follows:

Re-plannings allowance: Depending on available resources for plan adaptations, the model considers a maximum number of re-plannings B that can be implemented throughout the treatment. The analysis was performed for $B = 1, 2, 3$.

Decision epochs: Given a treatment period consisting of 33-35 fractions, the decision epochs were set at fractions 10, 15, 20, and 25. Prior studies have shown that anatomical changes are unlikely to happen very early during the treatment [21]; thus fraction 5 was omitted. Fraction 30 was also excluded due to its proximity to the end of treatment, with negligible impact on the total dose to the OARs.

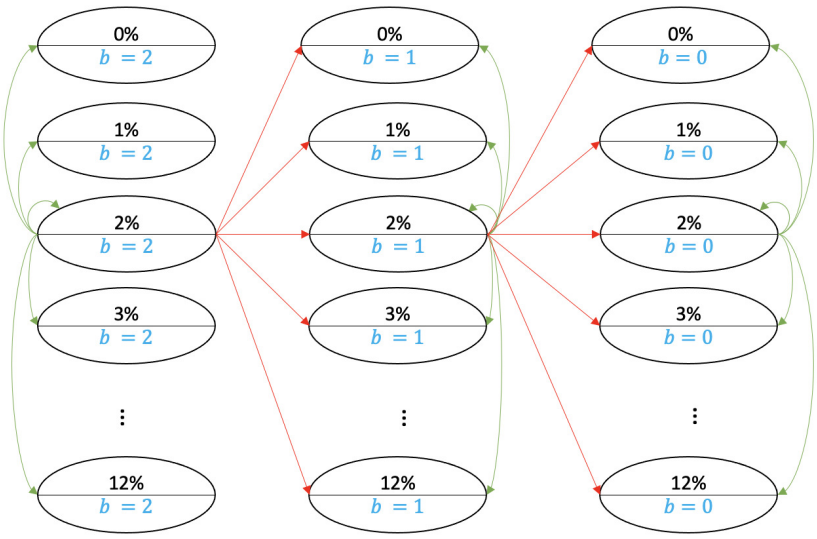

Figure 2: Markov Decision Process Model. The permissible number of re-plannings is 2 ($B = 2$). The states are shown by ellipses. ΔNTCP values are located in the upper half of the ellipses, while the lower halves contain the value of b (the number of remaining re-plannings). Transitions between states are shown by green arrows when the action is 'no re-planning' and by red arrows when the action is 're-planning.'

States: At each decision epoch, the state of the system was captured by the pair $(\Delta\text{NTCP}, b)$, where ΔNTCP denotes the deviation of treatment toxicity from the planned value at that time, and $b \leq B$ is the number of remaining re-plannings. For example, if the maximum permissible number of re-plannings is 2 ($B = 2$), and the clinician opts to implement a re-planning at fraction 10, then the state of the system at fraction 15 will have $b = 1$. The ΔNTCP ranges from 0% to 12% in the model (table 2).

Actions: At each decision epoch, two possible actions were included: (1) Re-planning, or (2) continue with the current plan (no re-planning). The stochastic transition of the toxicity state from one decision epoch to the next is a function of the action taken and is determined by the associated transition probabilities. Figure 2 illustrates the states of the MDP and possible transitions associated with each action, for the case that at most 2 re-plannings may be performed.

Transition Probabilities: The transition probabilities, governing the stochastic evolution of toxicity under each action, were estimated using the information presented in table 2. Under the 'no re-planning' action, the probabilities for transitions from fraction 0 to 10 and from fraction 10 to 15 were directly estimated based on the number of patients in each ΔNTCP category. For example, the probability of transitioning from ΔNTCP = 0% at fraction 0 to ΔNTCP = 1% at fraction 10 is $7/52 = 0.13$, as 7 patients out of 52 exhibited such a change in ΔNTCP from fraction 0 to fraction 10. The probabilities associated with the 'no re-planning' action are presented in Appendix B. It was assumed that transition probabilities from fraction 10 to 15 remained constant for subsequent decision epochs, due to the absence of reported ΔNTCP information

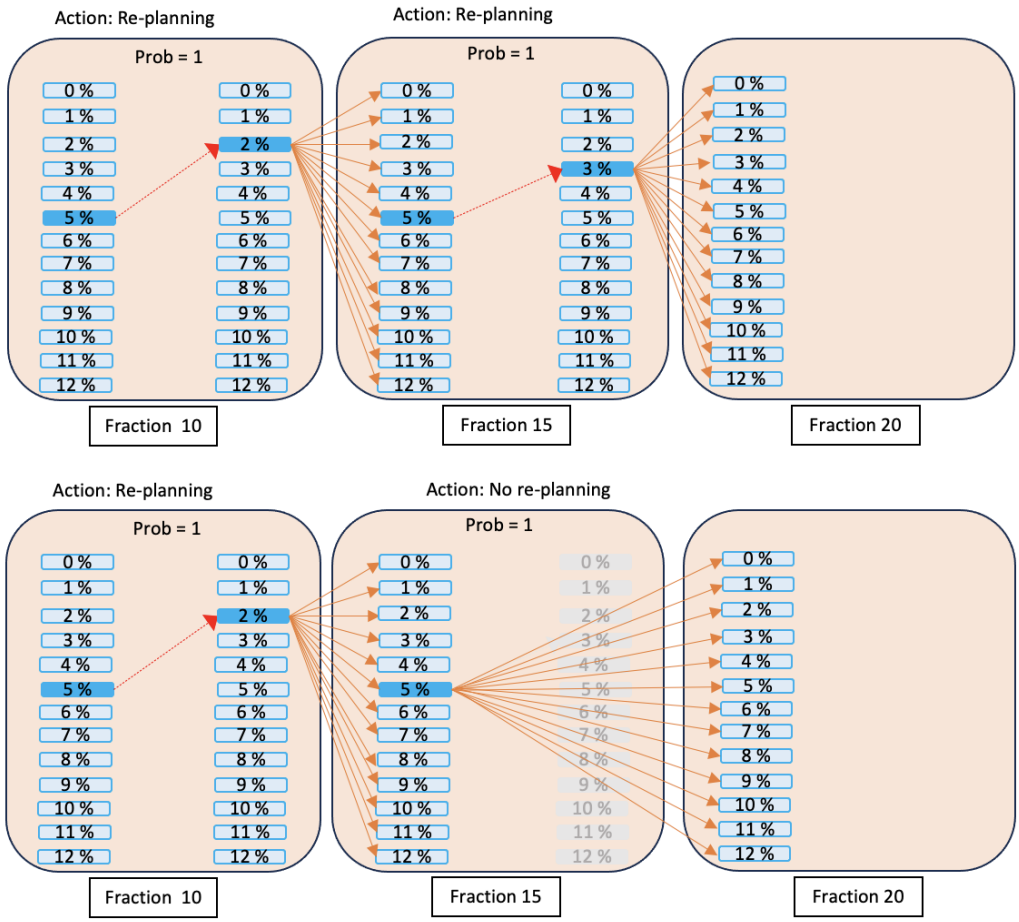

Figure 3: Effect of actions on the system transition. ΔNTCP values are shown in blue squares. Transitions under 're-planning' and 'no re-planning' are shown by arrows.

beyond fraction 15 by Heukelom et al. [21]. To model the impact of the 're-planning' action on transition probabilities, it was assumed that, at each decision epoch, the action immediately decreases ΔNTCP to a value proportional to the elapsed treatment time. For example, if the 're-planning' action is taken at fraction 10 for ΔNTCP = 5%, then the state of toxicity will immediately decrease to ΔNTCP = 2% at this fraction, as approximately one third of the treatment period has passed and the dose escalation will not continue through the rest of the treatment; see figure 3. Subsequently, the transition from fraction 10 to 15 is governed by the probabilities for ΔNTCP = 2%, calculated from tables 2. The probabilities associated with the 're-planning' action, as described above, are presented in Appendix B.

Rewards: For each set of consecutive actions taken at the decision epoch, the model considers the expected −ΔNTCP at the end of the treatment period (with respect to the transition probabilities) as the corresponding reward. The objective of the MDP is to maximize the expected reward by identifying an optimal set of actions, one at each decision epoch, as a function of the system's state. Because the rewards are defined by

Table 3: Optimal re-planning thresholds based on ΔNTCP and re-planning allowance.

Re-planning allowance (B)	1	2		3		
Number of remaining re-plannings (b)	1	2	1	3	2	1
ΔNTCP threshold at fraction 10	1%	1%	-	1%	-	-
ΔNTCP threshold at fraction 15	2%	2%	2%	2%	2%	-
ΔNTCP threshold at fraction 20	2%	2%	2%	2%	2%	2%
ΔNTCP threshold at fraction 25	4%	4%	4%	4%	4%	4%

negative values in the MDP model, smaller end-treatment ΔNTCP values translate to higher rewards.

3. Results

The MDP was solved using the `MDPtoolbox` of MATLAB [33], for $B = 1, 2, 3$. For each state (ΔNTCP, b) at each decision epoch, the software reports the optimal action ('re-planning' or 'no re-planning'). The optimal policy was a single-threshold policy. That is, if the optimal action for ΔNTCP $= x\%$ at a certain decision epoch was to re-plan, then for every other state with ΔNTCP $= y\% > x\%$ and the same b, the optimal action was also to re-plan.

When only one re-planning was allowed ($B = 1$), the optimal policy at fraction 10 was to re-plan for any ΔNTCP value greater than or equal to 1%. Subsequently, at fraction 15, this threshold increased to 2% and remained at 2% for fraction 20. At fraction 25, the minimum ΔNTCP required for a re-planning was 4%. These thresholds remained the same in the optimal policies for $B = 2, 3$. The results are summarized in table 3 and illustrated in figure 4 for $B = 3$. The MATLAB code and its outputs are publicly available at `https://github.com/fatemehhn/MDP-ART.git`.

4. Discussion

This study introduces the first — to our knowledge — application of the mathematically rigorous MDP methodology, to determine optimal timing of ART in HNC. Although we focused on HNC as a use case, the methodology described in this paper is applicable to other radiotherapy cancer sites where an adaptive scheduling regimen is desired for a 'budget' of re-plans with estimable NTCP metrics. By incorporating prior ΔNTCP data from serial CT-based OAR metrics from Heukelom et al. [21] within the proposed MDP model, we have successfully derived an optimal policy for treatment re-planning. The MDP model guides clinicians in determining the minimum values of ΔNTCP at fractions 10, 15, 20, and 25 for performing a re-planning, given a re-planning allowance of 1, 2, or 3 throughout the treatment.

The re-planning ΔNTCP threshold increases over time in the optimal policy, consistent with the diminishing impact of re-planning as the treatment progresses.

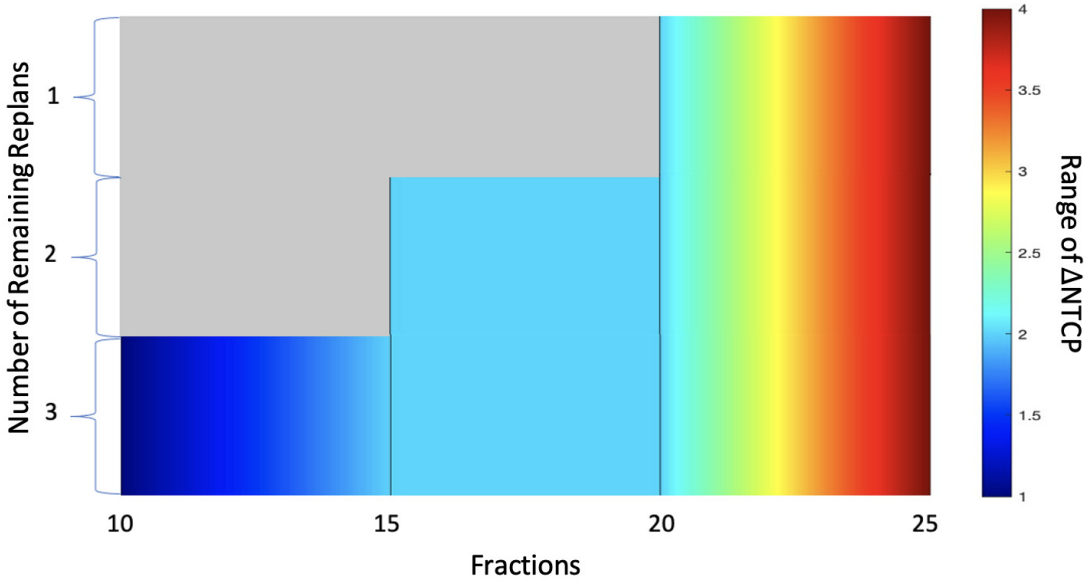

Figure 4: Optimal ΔNTCP thresholds for re-planning for $B = 3$.

These values are 1% at fraction 10, 2% at fractions 15 and 20, and 4% at fraction 25. Additionally, the results suggest optimality of re-planning for any changes in NTCP (ΔNTCP ≥ 1) at fraction 10. This supports the findings of Heukelom et al. [21], who identified fraction 10 as the optimal time for a single re-planning. Importantly, at a given fraction, the ΔNTCP thresholds remain the same for different number of re-plannings ($B = 1, 2, 3$); the re-planning allowance did not affect these thresholds. Furthermore, in cases where ΔNTCP at fraction 25 is below the 4% threshold, both options ('re-planning' or 'no re-planning') yield the same impact on the end-treatment ΔNTCP, indicating that re-planning does not result in an improvement.

The significance of a ΔNTCP of 4% or below lies in its potential impact on patient outcomes. While seemingly minor, even slight decreases in NTCP can have considerable implications for patient health and well-being. For instance, a reduction in severe toxicity such as osteoradionecrosis by just 4% could significantly enhance the quality of life and long-term survival prospects for patients. Moreover, customizing treatment to achieve such reductions underscores the importance of personalized care tailored to individual patient needs. By focusing on optimizing treatment outcomes at this level, healthcare practitioners can prioritize patient-centric approaches that aim to minimize treatment-related toxicity and maximize overall patient benefit.

We leveraged an existing CT-on-rails reference dataset [21] to objectively derive the ΔNTCP listed in the proposed MDP model. It is crucial to acknowledge the limitations regarding the generalizability of findings from this single-site retrospective in silico dataset. For instance, the in silico daily dose accumulation was not actively applied to individual patients, but rather calculated post hoc from a high-granularity CT-on-rails daily volumetric IGRT series. The CT-on-rails platform at MD Anderson utilized an in-

house custom-contructed intermediary localization and alienation software (CT-Assisted Targeting (CAT)) [34]. Consequently, there were instances where delivered geometric shifts were either unrecorded or unrecoverable, or clearly aberrant (such as extensive shift records representing an initial setup that was then revised after repositioning) during the secondary export of coordinate displacement to the commercial Record and Verify software (Mosaiq, Elekta AB). These discrepancies were subsequently omitted in the in silico model to streamline data, leading to conceptual gaps in the resultant NTCP modeling where these missing values were not accounted for. Furthermore, it is important to note that this modeled secondary dataset did not include adaptation or daily re-optimization of the initial daily dose in vivo. Consequently, the data presented in this paper should be viewed as a clinically approximate semi-synthetic illustrative use-case, rather than a definitive rationale for the large-scale implementation of the observed idealized re-planning thresholds across distinct operational platforms. Nonetheless, we believe that the resultant MDP model could be readily scaled using higher-quality prospective or observational cohort data for secondary validation. In essence, the data presented in this paper should be regarded as informative rather than definitive, and the individualized planning parameters suggested by MDP should be viewed as proof of concept rather than a formal criterion barring external validation.

In the prior work, Heukelom et al. [21] exclusively reported ΔNTCP for fractions 10 and 15, consistent with internal re-planning practices at MD Anderson Cancer Center based on data from a Phase II study by Maki et al. [35]. Consequently, for model extensibility in the current application, we have explicitly assumed transition probabilities remain stable for the subsequent epochs. This assumption introduces a known level of uncertainty that warrants consideration and is an area of future research, as it is unclear for specific OARs whether these transition states are indeed stable over therapy. Moreover, the MDP model stipulates weekly re-planning intervals on indexed fractions (e.g., fractions 10, 15, 20, 25, and 30) as a simplification for clarity of presentation reflective of our current adaptive protocols [22], but could readily be adapted to continuous daily fraction-based re-planning intervals.

The four NTCP models in table A1 are among the most currently used models to calculate the NTCP values for the considered toxicities: xerostomia, dysphagia, parotid gland dysfunction, and feeding tube dependency at 6 months post-treatment [21, 36]. With the advent of more recent NTCP models for HNC radiation therapy, e.g., [37], it is possible that new NTCP models could offer improved estimations. In addition, the presented results are based on data collected from 52 HNC patients. While we recognize the importance of sample size in calibrating MDPs, this sample size is considered substantial in HNC research, considering that HNC accounts for only about 4% of cancer cases in the United States [38]. Furthermore, our results are contingent upon the available CT-on-Rails data, and future research may benefit from incorporating higher-dimensional data (e.g., GTV/the clinical target volume (CTV) modifying approaches, MRI anatomic and/or biomarker data for TCP/NTCP) for a more extensive insight.

Nonetheless, the proposed MDP model for ART is clinically relevant,

mathematically rigorous, resource-aware, and scalable, and can be adjusted based on new OAR toxicity with reference NTCP values. Necessarily, the precision of the model relies on accurate calculations of NTCP, particularly when adhering to rigorous criteria that determine whether patients are suitable for or excluded from ART [39]. Despite the challenges and limitations, our study introduces novel contributions to the field of ART. Unlike previous works [16, 21], which primarily considered a single re-planning allowance, our optimization model extends its applicability to scenarios with multiple re-plannings. Furthermore, our optimal policy spans across fractions 10, 15, 20, and 25, representing an advancement beyond the limited scope of Heukelom et al. [21], which only reported results for fractions 10 and 15. Gan et al. [40] achieved optimal timing for re-planning in HNC radiation therapy by analyzing weekly dose data through semi-auto segmentation and the K-nearest-neighbour method. They constructed a dose deviation map to visualize differences between planned and actual doses, simulating different Adaptive Radiation Therapy scenarios. By evaluating accumulated dose differences before and after re-planning, the optimal timing for re-planning was determined. Our methodology differs in that we incorporate ΔNTCP and utilize it to develop an MDP model for determining the optimal timing for re-planning.

An aspect not explored in this study is the adaptation based on GTV or CTV modification, either for shrinking GTV/CTVs [22] or isotoxic boost approaches [41, 42]; we concentrated solely on OAR-based adaptation. Adapting based on GTV could open avenues for optimal re-plannings, potentially influencing NTCP and extending into scenarios such as Stereotactic Body RT [43]. This introduces a distinctive problem and solution space beyond the scope of our current investigation. Furthermore, we exclusively focused on optimizing the ART workflow within the context of photon therapy. Similar optimization methodologies could prove advantageous when exploring ART in the context of proton therapy, particularly in addressing setup variability reduction [44]. For this study, NTCP calculations were based on the 'plan of the day.' While our findings may vary with deformable dose registration, the operational implementation remains consistent. Future efforts should consider incorporating deformable dose registration to enhance the model's generalization.

Several surveys in both low/middle-income countries [45, 46] and high-income economies [45] have identified resource constraints as an impediment to ART implementation; the use of models such as our MDP provides a potential avenue for stratification of resource allocation. Put simply, with one re-plan allowed, almost all patients would be best served via re-planning early during treatment; however, as the budget of re-planning staff/technical/time resources expand, evidence-based personalized re-planning is potentiated by our MDP approach.

5. Conclusion

Our study introduced an MDP model to guide clinicians in determining the optimal timing for implementing patient-specific adaptive re-planning. This approach

incorporates ΔNTCP thresholds and considers varying total re-plannings. We also presented a novel in silico application and accompanying code specifically developed to attain improved ΔNTCP thresholds for consequential re-planning to alleviate toxicities throughout the course of treatment. Our methods have wide-ranging applicability, transcending specific cancer types and being adaptable to diverse institutional settings with limited resources. Additionally, our approach accommodates different OARs and NTCP models, emphasizing its versatility and potential for widespread implementation across a spectrum of clinical contexts.

Contributor Roles Taxonomy (CRediT) Attribution Statement

Conceptualization: F. Nosrat, C. Dede, L. B. McCullum, R. Garcia, A. S. Mohamed, J. G. Scott, J. E. Bates, B. A. McDonald, K. A. Wahid, M. A. Naser, R. He, A. C. Moreno, L. V. van Dijk, K. K. Brock, J. Heukelom, S. Hosseinian, M. Hemmati, A. J. Schaefer and C. D. Fuller; **Data curation:** F. Nosrat, C. Dede, L. B. McCullum, R. Garcia, A. S. Mohamed, B. A. McDonald, K. A. Wahid, J.H., S. Hosseinian, M. Hemmati and C. D. Fuller; **Formal analysis:** B. A. McDonald, K. A. Wahid, L. V. van Dijk, J. Heukelom, A. J. Schaefer and C. D. Fuller; **Funding acquisition:** J. Heukelom, A. J. Schaefer and C. D. Fuller; **Investigation:** F. Nosrat, C. Dede, L. B. McCullum, R. Garcia, S. Hosseinian, M. Hemmati, A. J. Schaefer and C. D. Fuller; **Methodology:** F. Nosrat, C. Dede, L. B. McCullum, R. Garcia, J. Heukelom, S. Hosseinian, M. Hemmati, A. J. Schaefer and C. D. Fuller; **Project administration:** F. Nosrat, C. Dede, L. B. McCullum, R. Garcia, R. He, S. Hosseinian, M. Hemmati, A. J. Schaefer and C. D. Fuller; **Resources:** A. S. Mohamed, B. A. McDonald, K. A. Wahid, M. A. Naser, R. He, L. V. van Dijk, K. K. Brock, , A. J. Schaefer and C. D. Fuller; **Software:** F. Nosrat, R. Garcia, S. Hosseinian, M. Hemmati; **Supervision:** A. J. Schaefer and C. D. Fuller; **Visualization:** F. Nosrat, C. Dede, L. B. McCullum, R. Garcia, S. Hosseinian, M. Hemmati; **Writing – original draft:** F. Nosrat, C. Dede, L. B. McCullum, R. Garcia, J. Heukelom, S. Hosseinian, M. Hemmati; **Writing - review & editing:** A. S. Mohamed, J. G. Scott, J. E. Bates, B. A. McDonald, K. A. Wahid, M. A. Naser, R. He., A. C. Moreno, L. V. van Dijk, K. K. Brock, J. Heukelom, S. Hosseinian, M. Hemmati, A. J. Schaefer and C. D. Fuller.

References

[1] N. A. Iacovelli et al. Role of IMRT/VMAT-based dose and volume parameters in predicting 5-year local control and survival in nasopharyngeal cancer patients. *Frontiers in Oncology*, **10**:518110, 2020.

[2] J. L. Barker Jr et al. Quantification of volumetric and geometric changes occurring during fractionated radiotherapy for head-and-neck cancer using an integrated CT/linear accelerator system. *International Journal of Radiation Oncology, Biology, Physics*, **59**(4):960–970, 2004.

[3] M. Beltran, M. Ramos, J. J. Rovira, S. Perez-Hoyos, M. Sancho, E. Puertas, S. Benavente, M. Ginjaume, and J. Giralt. Dose variations in tumor volumes and organs at risk during IMRT for head-and-neck cancer. *Journal of Applied Clinical Medical Physics*, **13**(6):3723, 2012.

[4] W. Chen, P. Bai, J. Pan, Y. Xu, and K. Chen. Changes in tumor volumes and spatial locations relative to normal tissues during cervical cancer radiotherapy assessed by cone beam computed tomography. *Technology in Cancer Research and Treatment*, 16(2):246–252, 2017.

[5] B. M. Beadle and A. W. Chan. The potential of adaptive radiotherapy for patients with head and neck cancer-too much or not enough? *JAMA Oncology*, 9(8):1064–1065, 2023.

[6] J. Castelli, A. Simon, C. Lafond, N. Perichon, B. Rigaud, E. Chajon, B. De Bari, M. Ozsahin, J. Bourhis, and R. de Crevoisier. Adaptive radiotherapy for head and neck cancer. *Acta Oncology*, **57**(10):1284–1292, 2018.

[7] M. Figen, D. Çolpan Öksüz, E. Duman, R. Prestwich, K. Dyker, K. Cardale, S. Ramasamy, P. Murray, and M. Şen. Radiotherapy for head and neck cancer: Evaluation of triggered adaptive replanning in routine practice. *Front Oncol*, **59**(4):960–970, 2020.

[8] K. Håkansson, E. Giannoulis, A. Lindegaard, J. Friborg, and I. Vogelius. Assessment of CBCT-based synthetic CT generation accuracy for adaptive radiotherapy planning. *Acta Oncologica (Stockholm, Sweden)*, **62**(11):1369–1374, 2023.

[9] E. Lavrova, M. D. Garrett, Y. F. Wang, C. Chin, C. Elliston, M. Savacool, M. Price, L. A. Kachnic, and D. P. Horowitz. Adaptive radiation therapy: A review of CT-based techniques. *Radiol Imaging Cancer*, **5**(4):e230011, 2023.

[10] C. J. O'Hara, D. Bird, B. Al-Qaisieh, and R. Speight. Assessment of CBCT-based synthetic CT generation accuracy for adaptive radiotherapy planning. *Journal of Applied Clinical Medical Physics*, **23**(11):e13737, 2022.

[11] K. K. Brock. Adaptive radiotherapy: Moving into the future. *Seminars in Radiation Oncology*, **29**(3):181–184, 2019.

[12] K. A. Wahid et al. Harnessing uncertainty in radiotherapy auto-segmentation quality assurance. *Physics and Imaging in Radiation Oncology*, **29**:100526, 2023.

[13] E. Huynh, A. Hosny, C. Guthier, S. F. Bitterman, D. A. Hass-Kogan, B. Kann, H. J. W. L. Aerts, and R. H. Mak. Artificial intelligence in radiation oncology. *Nature Reviews Clinical Oncology*, **17**:771–781, 2020.

[14] B. Bak, A. Skrobala, A. Adamska, J. Kazmierska, N. Jozefacka, T. Piotrowski, and J. Malicki. Criteria for verification and replanning based on the adaptive radiotherapy protocol "best for adaptive radiotherapy" in head and neck cancer. *Life*, **12**:722, 2022.

[15] S. Deng et al. Three-phase adaptive radiation therapy for patients with nasopharyngeal carcinoma undergoing intensity-modulated radiation therapy: Dosimetric analysis. *Technology in Cancer Research and Treatment*, **16**(6):910–916, 2017.

[16] G. K. Abou-Alfa et al. Phase II study of sorafenib in patients with advanced hepatocellular carcinoma. *Journal of Clinical Oncology: Official Journal of the American Society of Clinical Oncology*, **24**:4293–300, 2006.

[17] J. Castelli et al. Weekly adaptive radiotherapy vs standard intensity-modulated radiotherapy for improving salivary function in patients with head and neck cancer: A phase 3 randomized clinical trial. *JAMA Oncol.*, **9**(8):1056–1064, 2023.

[18] A. J. van de Schoot, D. Hoffmans, K. M. van Ingen, M. J. Simons, and J. Wiersma.

Characterization of Ethos therapy systems for adaptive radiation therapy: A multi-machine comparison. *Journal of Applied Clinical Medical Physics*, **24**:e13905, 2023.

[19] Varian Ethos. `https://www.varian.com`. Accessed: 2024-03-14.

[20] R. Avgousti, C. Antypas, C. Armpilia, F. Simopoulou, Z. Liakouli, P. Karaiskos, V. Kouloulias, E. Kyrodimos, L. A. Moulopoulos, and A. Zygogianni. Adaptive radiation therapy: When, how and what are the benefits that literature provides? *Cancer Radiotherapie : Journal de la Societe Francaise de Radiotherapie Oncologique*, **26**(4):622–636, 2022.

[21] J. Heukelom et al. Differences between planned and delivered dose for head and neck cancer, and their consequences for normal tissue complication probability and treatment adaptation. *Radiotherapy and Oncology*, **142**:100–106, 2020.

[22] H. Bahig et al. Magnetic resonance-based response assessment and dose adaptation in human papilloma virus positive tumors of the oropharynx treated with radiotherapy (MR-ADAPTOR): An R-IDEAL stage 2a-2b/Bayesian phase II trial. *Clinical and Translational Radiation Oncology*, **13**:19–23, 2018.

[23] E. A. Feinberg and A. Shwartz. *Handbook of Markov Decision Processes: Methods and Applications*. Springer, 2002.

[24] M. L. Puterman. *Markov Decision Processes: Discrete Stochastic Dynamic Programming*. Wiley-Interscience, 2005.

[25] J. R. Beck and S. G. Pauker. The Markov process in medical prognosis. *Medical Decision Making*, **3**(4):419–458, 1983.

[26] K. M. Kuntz, L. B. Russell, D. K. Owens, G. D. Sanders, T. A. Trikalinos, and J. A. Salomon. *Decision models in cost-effectiveness analysis. Cost-Effectiveness in Health and Medicine*. New York, NY: Oxford University Press, 2016.

[27] S. P. Ng et al. Surveillance imaging for patients with head and neck cancer treated with definitive radiotherapy: A partially observed Markov decision process model. *Cancer*, **126**(4):749–756, 2020.

[28] O. Alagoz, H. Hsu, A. J. Schaefer, and M. S. Roberts. Markov decision processes: A tool for sequential decision making under uncertainty. *Medical Decision Making: An International Journal of the Society for Medical Decision Making*, **30**(4):474–483, 2010.

[29] O. Alagoz, L. M. Maillart, A. J. Schaefer, and M. S. Roberts. The optimal timing of living-donor liver transplantation. *Management Science*, **50**(10):1420–30, 2004.

[30] B. T. Denton, M. Kurt, N. D. Shah, S. C. Bryant, and S. A. Smith. Optimizing the start time of statin therapy for patients with diabetes. *Medical Decision Making*, **29**(3):351–67, 2009.

[31] S. M. Shechter, M. D. Bailey, A. J. Schaefer, and M. S. Roberts. The optimal time to initiate HIV therapy under ordered health states. *Operations Research*, **56**(1):20–33, 2008.

[32] Introduction to Radiation Oncology. `https://doi.org/10.6084/m9.figshare.22582207.v1`. Accessed: 2024-02-24.

[33] The MathWorks Inc. MATLAB version: 9.13.0 (R2022b), 2022.

[34] L. Zhang, L. Dong, L. Court, H. Wang, M. Gillin, and R. Mohan. TU-EE-A4-05: Validation of CT-assisted targeting (CAT) software for soft tissue and bony target localization. *Journal of Applied Clinical Medical Physics*, **32**:2106–2106, 2005.

[35] R. G. Maki et al. Phase II study of sorafenib in patients with metastatic or recurrent sarcomas. *Journal of Clinical Oncology: Official Journal of the American Society of Clinical Oncology*, **27**(19):3133–3140, 2009.

[36] S. Stieb, A. Lee, L. V. van Dijk, S. Frank, C. D. Fuller, and P. Blanchard. NTCP modeling of late effects for head and neck cancer: A systematic review. *International Journal of Particle Therapy*, **8**(1):95–107, 2021.

[37] S. Hosseinian, M. Hemmati, C. Dede, T. C. Salzillo, L. V. van Dijk, A. S. R. Mohamed, S. Y. Lai, A. J. Schaefer, C. D. Fuller, Rice/MD Anderson Center for Operations Research in Cancer (CORC), and MD Anderson Head & Neck Cancer Symptom Working Group. Cluster-based toxicity estimation of osteoradionecrosis via unsupervised machine learning: Moving

beyond single dose-parameter normal tissue complication probability by using whole dose-volume histograms for cohort risk stratification. *International Journal of Radiation Oncology, Biology, Physics*, 2024.

[38] Head and Neck Cancer: Statistics. `https://www.cancer.net/cancer-types/head-and-neck-cancer/statistics`. Accessed: 2024-02-24.

[39] Y. Gan, J. A. Langendijk, A. van der Schaaf, L. van den Bosch, E. Oldehinkel, Z. Lin, S. Both, and C. L. Brouwer. An efficient strategy to select head and neck cancer patients for adaptive radiotherapy. *Radiotherapy and Oncology: Journal of the European Society for Therapeutic Radiology and Oncology*, **186**:109763, 2023.

[40] Y. Gan, J. A. Langendijk, E. Oldehinkel, Z. Lin, S. Both, and C. L. Brouwer. Optimal timing of re-planning for head and neck adaptive radiotherapy. *Journal of the European Society for Therapeutic Radiology and Oncology*, **194**:110145, 2024.

[41] J. Heukelom et al. Adaptive and innovative radiation treatment for improving cancer treatment outcome (ARTFORCE); a randomized controlled phase II trial for individualized treatment of head and neck cancer. *BMC Cancer*, **13**:84, 2013.

[42] A. D. Leeuw et al. Acute toxicity in ARTFORCE: A randomized phase III dose-painting trial in head and neck cancer. *International Journal of Radiation Oncology*Biology*Physics*, **114**(3):S98, 2022.

[43] I. Mohamad et al. The evolving role of stereotactic body radiation therapy for head and neck cancer: Where do we stand? *Cancers (Basel)*, **15**(20):5010, 2023.

[44] A. Lalonde, M. Bobić, G. C. Sharp, I. Chamseddine, B. Winey, and H. Paganetti. Evaluating the effect of setup uncertainty reduction and adaptation to geometric changes on normal tissue complication probability using online adaptive head and neck intensity modulated proton therapy. *Physics in Medicine and Biology*, **68**(11):115018, 2023.

[45] J. Bertholet et al. Patterns of practice for adaptive and real-time radiation therapy (POP-ART RT) part II: Offline and online plan adaption for interfractional changes. *Radiotherapy and Oncology: Journal of the European Society for Therapeutic Radiology and Oncology*, **153**:88–96, 2020.

[46] L. M. Yap, Z. Jamalludin, A. H. Ng, and N. M. Ung. A multi-center survey on adaptive radiation therapy for head and neck cancer in Malaysia. *Physical and Engineering Sciences in Medicine*, **46**(3):1331–1340, 2023.

[47] I. Beetz. NTCP models for patient-rated xerostomia and sticky saliva after treatment with intensity modulated radiotherapy for head and neck cancer: The role of dosimetric and clinical factors. *Radiother Oncology*, **105**(1):101–106, 2012.

[48] K. Wopken. Development of a multivariable normal tissue complication probability (NTCP) model for tube feeding dependence after curative radiotherapy/chemo-radiotherapy in head and neck cancer. *Radiother Oncology*, **113**(1):95–101, 2014.

[49] T. Dijkema, C. P. Raaijmakers, R. K. Ten Haken, J. M. Roesink, P. M. Braam, A. C. Houweling, M. A. Moerland, A. Eisbruch, and C. H. Terhaard. Parotid gland function after radiotherapy: The combined Michigan and Utrecht experience. *International Journal of Radiation Oncology, Biology, Physics*, **78**(2):449–453, 2010.

[50] Lyman J. T. Complication probability as assessed from dose-volume histograms. *Radiat Res Suppl*, **8**:S13–9, 1985.

[51] G. J. Kutcher and C. Burman. Calculation of complication probability factors for non-uniform normal tissue irradiation: The effective volume method. *International Journal of Radiation Oncology, Biology, Physics*, **16**(6):1623–1630, 1989.

[52] Christianen M. E. M. C. Predictive modelling for swallowing dysfunction after primary (chemo) radiation: Results of a prospective observational study. *Radiotherapy and Oncology: Journal of the European Society for Therapeutic Radiology and Oncology*, **105**(1):107–114, 2012.

Appendix A. NTCP Models

Table A1: The employed NTCP models for xerostomia, dysphagia, parotid gland dysfunction, and feeding tube dependency at 6 months post-treatment.

1. NTCP model for moderate to severe xerostomia at 6 months [47].

NTCP $= \left(1 + e^{-S}\right)^{-1}$, where
S = -1.443 + (mean dose to contralateral parotid * 0.047) + (baseline xerostomia score * 0.720).
Baseline xerostomia is 0 (none) or 1 (a bit).

2. NTCP model for physician rated feeding tube dependency at 6 months [48]

NTCP $= (1 + e^{-S})^{-1}$, where
S = -11.70 + (advanced T-stage * 0.43) + (moderate weight loss * 0.95)
+ (severe weight loss * 1.63) + (accelerated radiotherapy * 1.20) + (chemoradiation * 1.91)
+ (radiotherapy plus cetuximab * 0.56) + (mean dose PCM superior *0.071)
+ (mean dose PCM inferior * 0.034) + (mean dose contralateral parotid * 0.006)
+ (mean dose cricopharyngeal muscle * 0.023).
The dose variables are in Gy, and for all the other variables 0 (no) or 1 (yes) are filled in.

3. NTCP model for physician rated decreased salivary flow using the mean dose model [49, 50, 51].

NTCP $= \frac{1}{\sqrt{2\pi}} \int_{-\infty}^{u} e^{\frac{-t^2}{2}} dt$, where $u = \frac{D - TD_{50}}{mTD_{50}}$,
D is the mean parotid dose, TD_{50} is the dose resulting in 50% complication probability and m determines the slope of the model. The employed parameters were TD_{50}=39.9 Gy and $m = 0.4$.

4. NTCP model for dysphagia (grade 2–4 swallowing dysfunction according to the RTOG/EORTC Late Radiation Morbidity Scoring Criteria, physician rated 6 months after treatment) [52].

NTCP $= (1 + e^{-S})^{-1}$, where
$S = -6.09$+ (mean dose PCM superior * 0.057) + (mean dose supraglottic larynx * 0.037).

Appendix B. Transition Probabilities

Action 1: No re-planning

The natural transition probabilities from fraction 0 (pre-treatment) to fraction 10 were directly estimated using the information provided in table 2. For each ΔNTCP category, the ratio of the corresponding number of patients at fraction 10 to the total of 52 patients was taken as the associated transition probability. We note that all patients exhibit ΔNTCP = 0% at fraction 0. These probabilities apply only to the states with the same number of remaining re-plannings b, by the definition of the 'no re-planning' action. The transition probabilities are presented in table B1.

Table B1: Transition probabilities from fraction 0 (F0) to fraction 10 (F10) under 'no re-planning.'

ΔNTCP @ F10 → ΔNTCP @ F0 ↓	0%	1%	2%	3%	4%	5%	6%	7%	8%	9%	10%	11%	12%
0%	**0.50**	**0.13**	**0.08**	**0.11**	**0.04**	**0.04**	0.00	**0.02**	0.00	0.00	**0.02**	**0.02**	**0.04**

The natural transition probabilities from fraction 10 to fraction 15 were estimated in a similar manner. As the number of patients in each ΔNTCP category at fraction 15 were aggregated, a mapping from ΔNTCP categories at fraction 10 to those of fraction 15 was established. To ensure a feasible map, it was assumed that ΔNTCPs may slightly improve (1%) on its own, without intervention. The necessity of this assumption may be observed by the number of patients with ΔNTCP = 12% at fraction 10 and 15 in table 2; two patients exhibited ΔNTCP = 12% at fraction 10, while this number at fraction 15 was one patient. As no patient showed ΔNTCP = $6\%, 8\%, 9\%$ at fraction 10, it was assumed that the patients in these categories retain the same ΔNTCP at fraction 15 with probability 1. The transition probabilities are presented in table B2.

Table B2: Transition probabilities from fraction 10 (F10) to fraction 15 (F15) under 'no re-planning.' The same probabilities apply to subsequent transitions, i.e., from F15 to F20, from F20 to F25, and from F25 to end-treatment, under 'no re-planning.'

ΔNTCP @ F15 → ΔNTCP @ F10 ↓	0%	1%	2%	3%	4%	5%	6%	7%	8%	9%	10%	11%	12%
0%	**0.88**	0.00	0.12	0.00	0.00	0.00	0.00	0.00	0.00	0.00	0.00	0.00	0.00
1%	0.00	**1.00**	0.00	0.00	0.00	0.00	0.00	0.00	0.00	0.00	0.00	0.00	0.00
2%	0.00	**0.25**	**0.75**	0.00	0.00	0.00	0.00	0.00	0.00	0.00	0.00	0.00	0.00
3%	0.00	0.00	**0.50**	**0.33**	**0.17**	0.00	0.00	0.00	0.00	0.00	0.00	0.00	0.00
4%	0.00	0.00	0.00	0.00	**0.50**	0.00	**0.50**	0.00	0.00	0.00	0.00	0.00	0.00
5%	0.00	0.00	0.00	0.00	0.00	**0.50**	0.00	**0.50**	0.00	0.00	0.00	0.00	0.00
6%	0.00	0.00	0.00	0.00	0.00	0.00	**1.00**	0.00	0.00	0.00	0.00	0.00	0.00
7%	0.00	0.00	0.00	0.00	0.00	0.00	0.00	**1.00**	0.00	0.00	0.00	0.00	0.00
8%	0.00	0.00	0.00	0.00	0.00	0.00	0.00	0.00	**1.00**	0.00	0.00	0.00	0.00
9%	0.00	0.00	0.00	0.00	0.00	0.00	0.00	0.00	0.00	**1.00**	0.00	0.00	0.00
10%	0.00	0.00	0.00	0.00	0.00	0.00	0.00	0.00	0.00	0.00	**1.00**	0.00	0.00
11%	0.00	0.00	0.00	0.00	0.00	0.00	0.00	0.00	0.00	0.00	**1.00**	0.00	0.00
12%	0.00	0.00	0.00	0.00	0.00	0.00	0.00	0.00	0.00	0.00	0.00	**0.50**	**0.50**

Action 2: Re-planning

The impact of 're-planning' on transition probabilities at a specific fraction was modeled by presuming an immediate reduction in ΔNTCP to a proportion relative to the elapsed treatment time, followed by a natural transition governed by the probabilities associated with the reduced ΔNTCP. For instance, 're-planning' at fraction 10 when ΔNTCP is at 5% results in an immediate decrease to ΔNTCP = 2%, reflecting that about one-third of the treatment has been completed. This is then followed by a transition (from F10 to F15) according to the probabilities associated with ΔNTCP = 2% @ F10 in table B2. These probabilities are presented in the following tables. We note that the earliest decision epoch for 're-planning' is fraction 10.

Table B3: Transition probabilities from fraction 10 (F10) to fraction 15 (F15) under 're-planning.'

ΔNTCP @ F15 → ΔNTCP @ F10 ↓	0%	1%	2%	3%	4%	5%	6%	7%	8%	9%	10%	11%	12%
0%	**0.88**	0.00	**0.12**	0.00	0.00	0.00	0.00	0.00	0.00	0.00	0.00	0.00	0.00
1%	**0.88**	0.00	**0.12**	0.00	0.00	0.00	0.00	0.00	0.00	0.00	0.00	0.00	0.00
2%	0.00	**1.00**	0.00	0.00	0.00	0.00	0.00	0.00	0.00	0.00	0.00	0.00	0.00
3%	0.00	**1.00**	0.00	0.00	0.00	0.00	0.00	0.00	0.00	0.00	0.00	0.00	0.00
4%	0.00	**1.00**	0.00	0.00	0.00	0.00	0.00	0.00	0.00	0.00	0.00	0.00	0.00
5%	0.00	**0.25**	**0.75**	0.00	0.00	0.00	0.00	0.00	0.00	0.00	0.00	0.00	0.00
6%	0.00	**0.25**	**0.75**	0.00	0.00	0.00	0.00	0.00	0.00	0.00	0.00	0.00	0.00
7%	0.00	**0.25**	**0.75**	0.00	0.00	0.00	0.00	0.00	0.00	0.00	0.00	0.00	0.00
8%	0.00	0.00	**0.50**	**0.33**	**0.17**	0.00	0.00	0.00	0.00	0.00	0.00	0.00	0.00
9%	0.00	0.00	**0.50**	**0.33**	**0.17**	0.00	0.00	0.00	0.00	0.00	0.00	0.00	0.00
10%	0.00	0.00	**0.50**	**0.33**	**0.17**	0.00	0.00	0.00	0.00	0.00	0.00	0.00	0.00
11%	0.00	0.00	0.00	0.00	**0.50**	0.00	**0.50**	0.00	0.00	0.00	0.00	0.00	0.00
12%	0.00	0.00	0.00	0.00	**0.50**	0.00	**0.50**	0.00	0.00	0.00	0.00	0.00	0.00

Table B4: Transition probabilities from fraction 15 (F15) to fraction 20 (F20) under 're-planning.'

ΔNTCP @ F20 → ΔNTCP @ F15 ↓	0%	1%	2%	3%	4%	5%	6%	7%	8%	9%	10%	11%	12%
0%	**0.88**	0.00	**0.12**	0.00	0.00	0.00	0.00	0.00	0.00	0.00	0.00	0.00	0.00
1%	0.00	**1.00**	0.00	0.00	0.00	0.00	0.00	0.00	0.00	0.00	0.00	0.00	0.00
2%	0.00	**1.00**	0.00	0.00	0.00	0.00	0.00	0.00	0.00	0.00	0.00	0.00	0.00
3%	0.00	**0.25**	**0.75**	0.00	0.00	0.00	0.00	0.00	0.00	0.00	0.00	0.00	0.00
4%	0.00	**0.25**	**0.75**	0.00	0.00	0.00	0.00	0.00	0.00	0.00	0.00	0.00	0.00
5%	0.00	0.00	**0.50**	**0.33**	**0.17**	0.00	0.00	0.00	0.00	0.00	0.00	0.00	0.00
6%	0.00	0.00	**0.50**	**0.33**	**0.17**	0.00	0.00	0.00	0.00	0.00	0.00	0.00	0.00
7%	0.00	0.00	0.00	0.00	**0.50**	0.00	**0.50**	0.00	0.00	0.00	0.00	0.00	0.00
8%	0.00	0.00	0.00	0.00	**0.50**	0.00	**0.50**	0.00	0.00	0.00	0.00	0.00	0.00
9%	0.00	0.00	0.00	0.00	0.00	**0.50**	0.00	**0.50**	0.00	0.00	0.00	0.00	0.00
10%	0.00	0.00	0.00	0.00	0.00	**0.50**	0.00	**0.50**	0.00	0.00	0.00	0.00	0.00
11%	0.00	0.00	0.00	0.00	0.00	0.00	**1.00**	0.00	0.00	0.00	0.00	0.00	0.00
12%	0.00	0.00	0.00	0.00	0.00	0.00	**1.00**	0.00	0.00	0.00	0.00	0.00	0.00

Table B5: Transition probabilities from fraction 20 (F20) to fraction 25 (F25) under 're-planning.'

ΔNTCP @ F25 → ΔNTCP @ F20 ↓	0%	1%	2%	3%	4%	5%	6%	7%	8%	9%	10%	11%	12%
0%	**0.88**	0.00	**0.12**	0.00	0.00	0.00	0.00	0.00	0.00	0.00	0.00	0.00	0.00
1%	0.00	**1.00**	0.00	0.00	0.00	0.00	0.00	0.00	0.00	0.00	0.00	0.00	0.00
2%	0.00	**1.00**	0.00	0.00	0.00	0.00	0.00	0.00	0.00	0.00	0.00	0.00	0.00
3%	0.00	**0.25**	**0.75**	0.00	0.00	0.00	0.00	0.00	0.00	0.00	0.00	0.00	0.00
4%	0.00	0.00	**0.50**	**0.33**	**0.17**	0.00	0.00	0.00	0.00	0.00	0.00	0.00	0.00
5%	0.00	0.00	**0.50**	**0.33**	**0.17**	0.00	0.00	0.00	0.00	0.00	0.00	0.00	0.00
6%	0.00	0.00	0.00	0.00	**0.50**	0.00	**0.50**	0.00	0.00	0.00	0.00	0.00	0.00
7%	0.00	0.00	0.00	0.00	0.00	**0.50**	0.00	**0.50**	0.00	0.00	0.00	0.00	0.00
8%	0.00	0.00	0.00	0.00	0.00	**0.50**	0.00	**0.50**	0.00	0.00	0.00	0.00	0.00
9%	0.00	0.00	0.00	0.00	0.00	0.00	**1.00**	0.00	0.00	0.00	0.00	0.00	0.00
10%	0.00	0.00	0.00	0.00	0.00	0.00	0.00	**1.00**	0.00	0.00	0.00	0.00	0.00
11%	0.00	0.00	0.00	0.00	0.00	0.00	0.00	**1.00**	0.00	0.00	0.00	0.00	0.00
12%	0.00	0.00	0.00	0.00	0.00	0.00	0.00	0.00	**1.00**	0.00	0.00	0.00	0.00

Table B6: Transition probabilities from fraction 25 (F25) to end-treatment under 're-planning.'

ΔNTCP @ end → ΔNTCP @ F25 ↓	0%	1%	2%	3%	4%	5%	6%	7%	8%	9%	10%	11%	12%
0%	**0.88**	0.00	**0.12**	0.00	0.00	0.00	0.00	0.00	0.00	0.00	0.00	0.00	0.00
1%	0.00	**1.00**	0.00	0.00	0.00	0.00	0.00	0.00	0.00	0.00	0.00	0.00	0.00
2%	0.00	**0.25**	**0.75**	0.00	0.00	0.00	0.00	0.00	0.00	0.00	0.00	0.00	0.00
3%	0.00	0.00	**0.50**	**0.33**	**0.17**	0.00	0.00	0.00	0.00	0.00	0.00	0.00	0.00
4%	0.00	0.00	**0.50**	**0.33**	**0.17**	0.00	0.00	0.00	0.00	0.00	0.00	0.00	0.00
5%	0.00	0.00	0.00	0.00	**0.50**	0.00	**0.50**	0.00	0.00	0.00	0.00	0.00	0.00
6%	0.00	0.00	0.00	0.00	0.00	**0.50**	0.00	**0.50**	0.00	0.00	0.00	0.00	0.00
7%	0.00	0.00	0.00	0.00	0.00	0.00	**1.00**	0.00	0.00	0.00	0.00	0.00	0.00
8%	0.00	0.00	0.00	0.00	0.00	0.00	0.00	**1.00**	0.00	0.00	0.00	0.00	0.00
9%	0.00	0.00	0.00	0.00	0.00	0.00	0.00	0.00	**1.00**	0.00	0.00	0.00	0.00
10%	0.00	0.00	0.00	0.00	0.00	0.00	0.00	0.00	**1.00**	0.00	0.00	0.00	0.00
11%	0.00	0.00	0.00	0.00	0.00	0.00	0.00	0.00	0.00	**1.00**	0.00	0.00	0.00
12%	0.00	0.00	0.00	0.00	0.00	0.00	0.00	0.00	0.00	0.00	**1.00**	0.00	0.00